LONGITUDINAL WAVE PRECURSOR SIGNAL FROM AN OPTICALLY PENETRATING THERMOELASTIC LASER SOURCE

R. J. Conant
Department of Mechanical Engineering
Montana State University, Bozeman, MT 59717

K. L. Telschow
Idaho National Engineering Laboratory
EG&G Idaho, Inc., Idaho Falls, ID 83415-2209

INTRODUCTION

The thermoelastic laser ultrasonic source depends on the optical absorption of energy at the sample surface to produce a volumetric expansion. This paper presents the results of calculations and measurements on the effects of optical penetration of the laser beam into the sample and the elastic waveforms produced. A central result is prediction of a sharp longitudinal waveform that precedes the main waveform and is very similar to that observed with an ablative source (normal point force). The shape of this precursor signal is strongly dependent on the optical penetration depth of the material. A basic explanation of the origin of the precursor signal is given in terms of a one-dimensional model using point sources imbedded within the material. Experimental measurements on a material with a substantial optical penetration depth directly confirm calculations using 2-D integral transform techniques by taking into account the temperature variation with depth.

Recently, much effort has been concentrated on developing pulsed lasers as sources of ultrasonic waves for noncontacting measurements [1,2]. The results to date are very promising in that the laser is an efficient and very controllable source. A feature of the elastic wave produced that has been found useful for characterizing microstructural effects is the presence of a spiked longitudinal pulse preceding the main waveform. This spike can be produced by ablation of material from the sample surface. However, it is also possible to produce this feature with a subsurface thermoelastic source produced by either thermal diffusion or optical penetration, both of which produce an effective subsurface source in the material. This investigation specifically studies the generation of this spike for materials where the optical penetration depth is significant. The goal of this work was to quantitatively characterize and explain the waveforms produced by the laser source through actual measurement of displacements and calculations based on thermoelastic models.

EXPERIMENTAL MEASUREMENTS

The experimental arrangement is shown in Fig. 1. The sample materials were stainless steel, which served as a material with essentially zero optical penetration depth, and neutral density filters (NDF) [3] with a variety of optical penetration depths. All the samples were flat plates ~2.5 to 3.5 mm thick. The detector used was a capacitive transducer, which directly recorded the surface displacement on the side opposite from where the laser pulse was absorbed. All the NDF glass plates were coated with platinum on the capacitive detector side to serve as the grounding electrode. The results reported here are for the detector on epicenter from the laser beam. Fig. 1 shows the overall geometry, polarity of the measured displacements, and the optical penetration depth (the distance at which the incident intensity drops to 1/e of its surface value). The laser beam profile was assumed Gaussian for the purposes of the calculation. Experimentally, the beam approximated a Gaussian with a central maximum of intensity and much lesser intensity toward the outer beam radius.

Fig. 2 shows the measured waveforms for the stainless steel sample [SS] and one of the NDF samples [A], which exhibited a relatively large optical absorption. The primary effect of the laser source on Sample [SS] is to produce a negative displacement starting at the longitudinal wave arrival time. This motion is brought back toward the equilibrium line by the arrival of the transverse wave portion to the initial longitudinal expansion. For relatively thin plates, as used here, the subsequent motion represents a significant excitation of low frequency plate mode vibrations, which continue for several milliseconds. Sample [A] exhibits an optical penetration depth of about 11.4% of its thickness. Its waveform, as seen in Fig. 2, is similar to

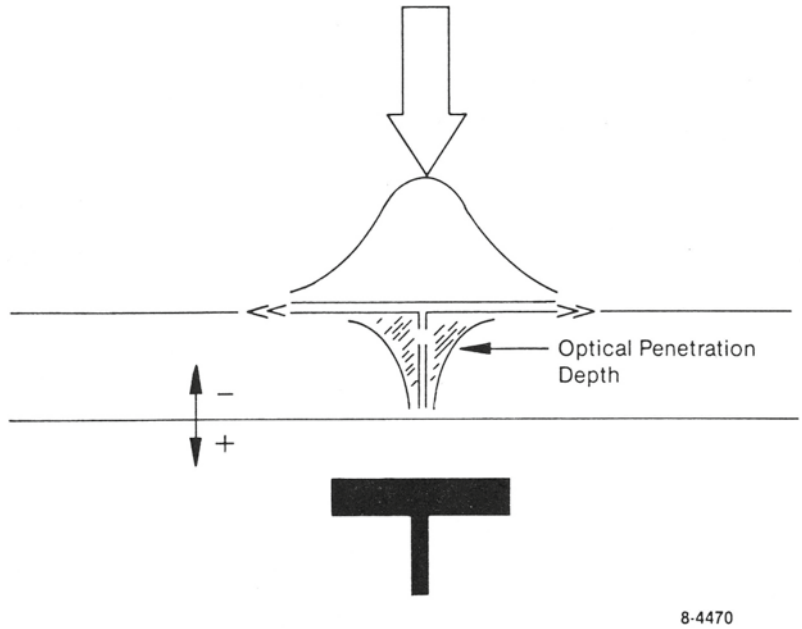

Fig. 1. Experimental arrangement showing the pulsed laser source and the capacitive surface displacement detector.

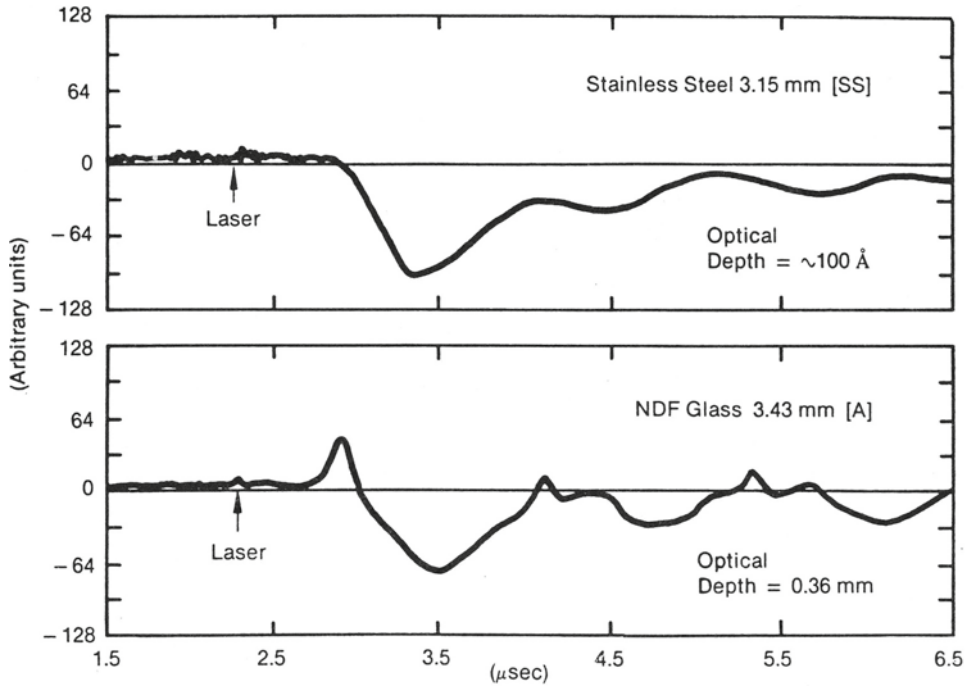

Fig. 2. Normal surface displacement from absorption of the laser pulse. Note the sharp positive-going displacement (precursor) for the neutral density filter (NDF) Sample [A] as compared with the relatively nonabsorbing stainless steel plate.

that for [SS] except that a positive spike appears in the waveform somewhat before the longitudinal arrival time. This is the precursor signal and its magnitude increases with the optical penetration depth. For penetration depths on the order of the plate thickness, the shape of the precursor is altered markedly and a positive displacement is seen immediately when the laser pulse is absorbed. As the following calculations show, the shape of this precursor signal is strongly determined by the material's optical penetration depth.

ONE-DIMENSIONAL MODEL

Much about the precursor signal can be understood from investigating a one-dimensional model describing the thermoelastic expansion and waveform generation. This model can be solved explicitly in closed form. The plate is approximated as an infinite layer of thickness (2h) with the laser source above and the capacitor detector below as in Fig. 1. The laser beam is absorbed exponentially from the top surface producing an internal temperature distribution according to

$$T(z,t) = T_o \exp[-\eta(1+z)]\ H(t)$$

where z is measured in units of thickness and η is the thickness divided by the optical penetration depth [4]. Here it is assumed that the laser pulse duration is too short for significant thermal diffusion to occur on the time scale of the measurement (μs); therefore, time dependence is governed by the Heaviside function H(t). It is also convenient to measure time in dimensionless units given by $t = C_S\ t_{actual}/h$, with C_S the shear wave speed in the material.

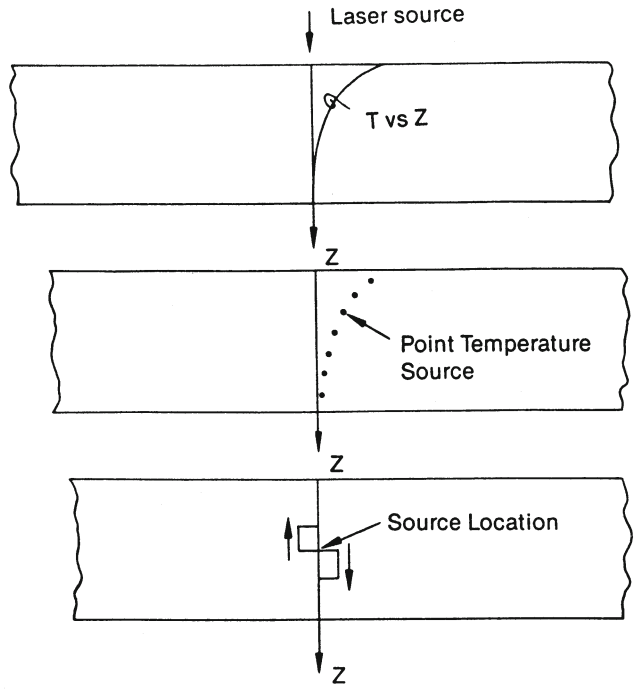

Fig. 3. Visualization of the optically penetrating laser source as a collection of point expansion sources, along with the two waveforms produced from each point source.

The temperature distribution can be described by a collection of point expansion sources (see Fig. 3) each of which generates a forward and backward propagating longitudinal wave whose amplitude is proportional to the value of the temperature at that point. The wave generated by the temperature source closest to the bottom surface (z = 1) reaches that surface first, but its amplitude is small. It is followed by the wave generated at the temperature source point that is next closest and whose amplitude is a little larger, and so on. Thus, the displacement of the bottom surface starts out very small but increases rapidly as the waves generated by the temperature sources closer to the top surface arrive. The net waveform results from the superposition of the forward and time delayed backward traveling waves. Fig. 4 shows the net displacement at the bottom surface for this model. It is apparent that only a positive spike is produced as a result of the heating with depth caused by the finite optical penetration into the material. Also the precursor pulse shape reflects the source temperature distribution in the material. As the optical penetration depth of materials decreases to zero, the amplitude of the precursor signal decreases to zero also. Therefore, no observable precursor is predicted for materials such as stainless steel, as in Fig. 2, where the penetration depth is only angstroms thick.

TWO-DIMENSIONAL MODEL

The more general problem can be treated as two-dimensional if rotational symmetry is assumed about the laser beam axis [5]. Now the radial heating function is taken as Gaussian, yielding the temperature as

$$T(r,z,t) = T_o \exp[-r^2/a^2] \exp[-\eta(1+z)] H(t)$$

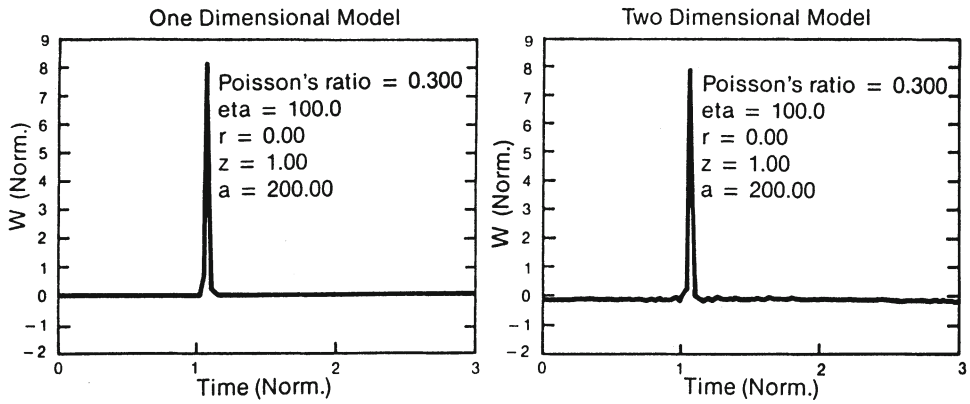

Fig. 4. Positive displacement pulse resulting from the buried sources as calculated from the one-dimensional model [top] and from the wide beam width limit of the two-dimensional model, using 300 modes and 8 quadrature points.

where the beam radius is (a), measured in units of the plate thickness. The uncoupled dimensionless equations of thermoelasticity are

$$(1/r)(r\Phi_{,r})_{,r} + \Phi_{,zz} = (C_S/C_L^2)\ddot{\Phi} + [(1+\nu)/(1-\nu)]\alpha T$$

$$(1/r)(r\Psi_{,r})_{,r} - (1/r^2)\Psi + \Psi_{,zz} = \ddot{\Psi}$$

where Φ and Ψ are the Lame potentials, ν is Poisson's ratio, and α is the coefficient of thermal expansion. The displacement components, U and W in the radial and axial directions respectively, are related to the potentials by

$$U = \Phi_{,r} - \Psi_{,z} \quad \text{and} \quad W = \Phi_{,z} + (1/r)(r\Psi)_{,r} .$$

On the layer surfaces, z = +/-h, the normal and shear stresses must vanish. The solution to these equations follows the treatment of Reference [5], except that we now concentrate on the waveform displacements. The solution proceeds by using the Laplace transform to eliminate dependence on time, then the Hankel transform for the radial coordinate. After solving the resulting ordinary differential equations, the Laplace transform is inverted by residue theory. Since the transformed expressions for the displacement contain an infinite number of simple poles, the inversion results in an infinite series of plate propagation modes, both symmetric and antisymmetric. Inversion of the Hankel transforms results in formal expressions for the displacements as a function of position and time in the form of infinite integrals, which are evaluated numerically. Formally, the normalized displacement W is given by

$$W(r,z,t) \equiv AW_{actual}/h = \int_0^\infty \kappa W_o(\kappa,z,t) J_o(\kappa r)\, d\kappa$$

where $A = [(1+\nu)/(1-\nu)\alpha T_o a^2]^{-1}$, and

$$W_o(\kappa,z,t,) = W_{static}(\kappa,z,t) - 2\sum_{n=1}^{\infty} \exp[-\kappa^2 a^2/4] M_s(\Omega_{ns},\kappa,z)\cos(\Omega_{ns} t)$$

$$- 2\sum_{n=1}^{\infty} \exp[-\kappa^2 a^2/4] M_a(\Omega_{na},\kappa,z)\cos(\Omega_{na} t)$$

which is a sum over all the symmetric and antisymmetric modes of the plate. The dispersion relation for the symmetric mode is given below; a similar relation exists for the antisymmetric modes.

$$(\kappa^2 - \beta^2)\sin(\beta)\cos(\gamma) + 4\eta^2\gamma\beta\sin(\gamma)\cos(\beta) = 0$$

where $\gamma \equiv [(C_S^2/C_L^2)\Omega_s^2 - \kappa^2]^{1/2}$, and $\beta \equiv (\Omega_s^2 - \kappa^2)^{1/2}$.

With $y = \kappa^2 a^2/4$, integrals of the form $\int \exp[-\kappa^2 a^2/4] f(\kappa) d\kappa$

can be written as $\int \exp[-y] g(y) dy$, for which Gaussian quadrature formulae are available. Thus, the numerical integration can be carried out in a straightforward manner.

Fig. 5 shows the calculated displacement W at the epicenter position for a beam diameter equal to the plate thickness, an optical penetration depth of 1% of the plate thickness, and a Poisson's ratio of 0.30. For the dimensionless time units used, the shear wave arrival time is at $t = 2$ and for the chosen Poisson's ratio the longitudinal wave arrival time is $t = 1.07$. Because of the sharp rise in the displacement that occurs near the longitudinal arrival time, a large number of modes must be used in the summations. For Fig. 5, 450 symmetric and antisymmetric modes were calculated resulting in good qualitative agreement with experiment. As the beam radius gets very large, the two-dimensional solution approaches the one-dimensional solution as shown by comparing the two waveforms in Fig. 4.

RESULTS AND DISCUSSION

A direct comparison between the experimental measurement for the NDF Sample [A] and the appropriate two-dimensional calculation is shown in Fig. 6. Here, the the two graphs are normalized by overlapping the precursor peaks in time and adjusting the vertical scale so the maximum negative displacements agree. Most of the essential features of the two graphs agree. The precursors rise approximately exponentially and fall abruptly to be followed by the negative thermoelastic expansion. Both curves show a shift to later times of the transverse wave arrival time, although in the experiment this shift is larger. The origin of the broader precursor peak and the later transverse wave arrival time is thought to be from the finite bandwidth (~70 MHz) of the capacitive detector.

CONCLUSIONS

Due to optical penetration into the material, a positive displacement longitudinal precursor waveform to the negative displacement thermoelastic waveform is produced within the material. The precursor waveform results from the fact that with optical penetration, expansion sources exist within the material. The shape of this waveform directly reflects the distribution and magnitude of sources with depth in the material. The combined waveform of these imbedded sources produces a

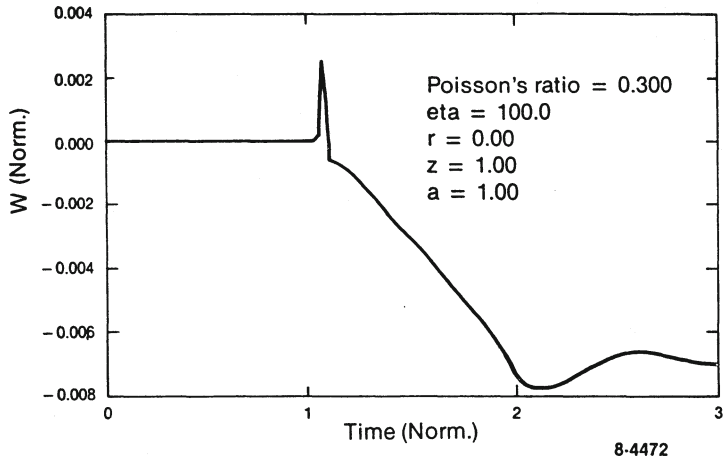

Fig. 5. Displacement (normalized) as a function of time (normalized) for a relatively small optical penetration depth (1% of plate thickness) as calculated from the two-dimensional model, using 450 modes and 8 quadrature points.

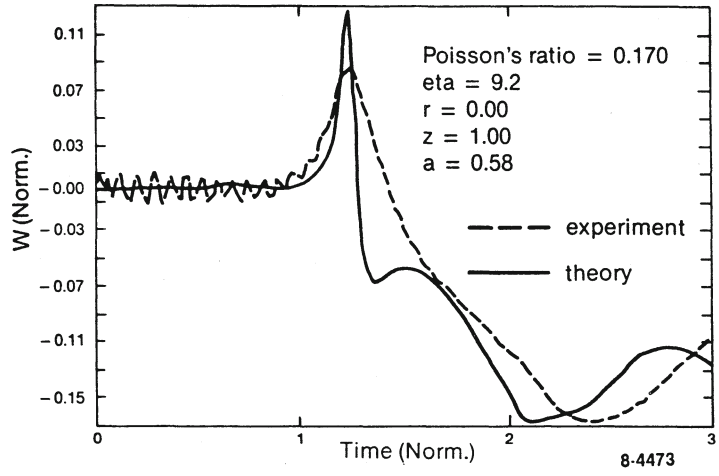

Fig. 6. Comparison between the experimentally measured surface displacement and that calculated for an NDF with optical penetration depth of 11.4% of the plate thickness. The signal amplitudes are normalized so that the maximum negative displacements are equal. 450 modes and 8 quadrature points were used for the calculation.

rapidly rising positive displacement pulse, which can be used for material analysis (attenuation or velocity) since it contains a significant amount of high frequency. Direct experimental measurement and analytical calculation confirm the expectations based on point source models and have been shown to agree with each other. These results are directly applicable to semitransparent ceramic materials that are being evaluated with laser ultrasonic techniques.

ACKNOWLEDGMENT

The authors would like to thank J. Jolley for assistance in preparing the platinum coated samples and N. Boyce for constructing the capacitive detector. The assistance of T. O'Brien in recording the data is greatly appreciated. This work was supported by the Department of Interior's Bureau of Mines under Contract No. J0134035 through Department of Energy contract No. DE-AC07-76ID01570.

REFERENCES

1. C. B. Scruby, R. L. Smith and B. C. Moss, "Microstructural Monitoring by Laser-Ultrasonic Attenuation and Forward Scattering," NDT International, 19, 307-313, 1986.

2. C. B. Scruby, R. J. Dewhurst, D. A. Hutchins and S. B. Palmer, "Laser Generation of Ultrasound in Metals," in Research Techniques in Nondestructive Testing, ed. R. S. Sharp, 5, pp. 281-327, Academic Press, New York, 1982.

3. Ealing Optics Co., Pleasant Street, South Natick, MA, 01760.

4. J. F. Ready, Effects of High-Power Laser Radiation," Academic Press, Inc., New York, 1971.

5. C. Sve and J. Miklowitz, "Thermally Induced Stress Waves in an Elastic Layer," J. Appl. Mech., 40, 161-167, 1973.